CHAPTER 05 Experimental study of FB-TIG welding

5.1 Preamble

This chapter discuss the purpose of adopting FB-TIG welding process. To apply this novel variant of A-TIG, optimal flux gap and best flux is identified by comparing macrostructure of weld joint. Furthermore, the chapter discuss the effect of different heat input on macrostructure, microstructure and mechanical properties (tensile strength, microhardness) on FB-TIG weld joint.

5.2 Purpose of adopting Flux Bounded TIG (FB-TIG) welding

Activated TIG (A-TIG) welding successfully increases the penetration capability along with mechanical properties in 6mm thick 2205 DSS as reported in chapter 4. However, in A-TIG welding, applied activated flux offers resistance to arc. Therefore, the energy required for melting the flux reduces the welding efficiency. It is difficult to track the weld line due to the complete convergence of the weld line with flux. Moreover, after welding entrapped flux particles create a poor weld bead surface appearance as shown in Figure 5.1.

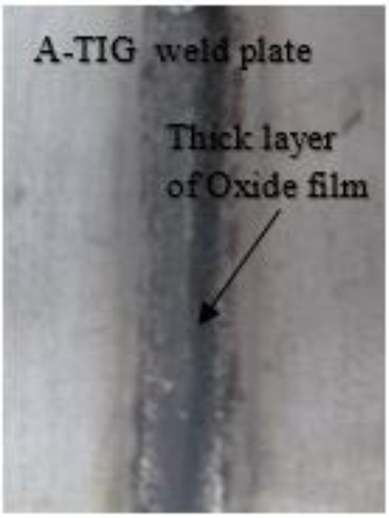

Figure 5.1 A-TIG weld surface

This drawback of A-TIG welding is eliminated by another novel chronological advance process called Flux Bounded TIG welding (FB-TIG), along with adopting the benefits of A-TIG welding (Singh, Dey, & Rai, 2017; Pandya, Badgujar, & Ghetiya, 2021). Therefore, further investigation is on 2205 DSS is carried out by FB-TIG welding process.

5.3 Experimentation of FB-TIG weld

In the current study, experiments are performed on 100 × 100 × 6 mm 2205 DSS. To identify the optimal flux gap, the flux layer gap is varied from 2 mm to 7 mm in the step of 1 mm. The weld area is polished and clean with acetone to eliminate the surface contaminants. Before welding, acetone is mixed in SiO_2 flux to from paste-like consistency. This mixture is spread using a paint brush leaving a predetermined weld centreline. The uniform flux thickness of 0.16 mm is maintained along the weld line as shown in Figure 5.2. FB-TIG butt welding is performed using a developed fixture at a constant welding current of 185 amps, welding speed of 120 mm/min. The other constant parameters such as shielding gas, flow rate, arc length, etc. are already mentioned in Table 4.2. After finding the optimal flux gap with SiO_2 flux, experiments are performed with other single component fluxes such as TiO_2 and Cr_2O_3 at the same welding parameters to identify the best single-component flux. To analyze the effect of heat input, the welding current is varying from 160 amps to 235 amps at the interval of 25 amps with optimal flux gap and best flux combinations. During the welding heat, input is calculated using equation (5.1). Furthermore, TIG welding is performed on the aforementioned process parameters. The characteristics of the FB-TIG weld joint are compared with TIG weld joints.

$$\text{H}eat\ input = \frac{Voltage(V) \times Current(amps) \times 60}{\text{Torch}\ speed(mm/min) \times 1000} \text{ KJ/mm} \tag{5.1}$$

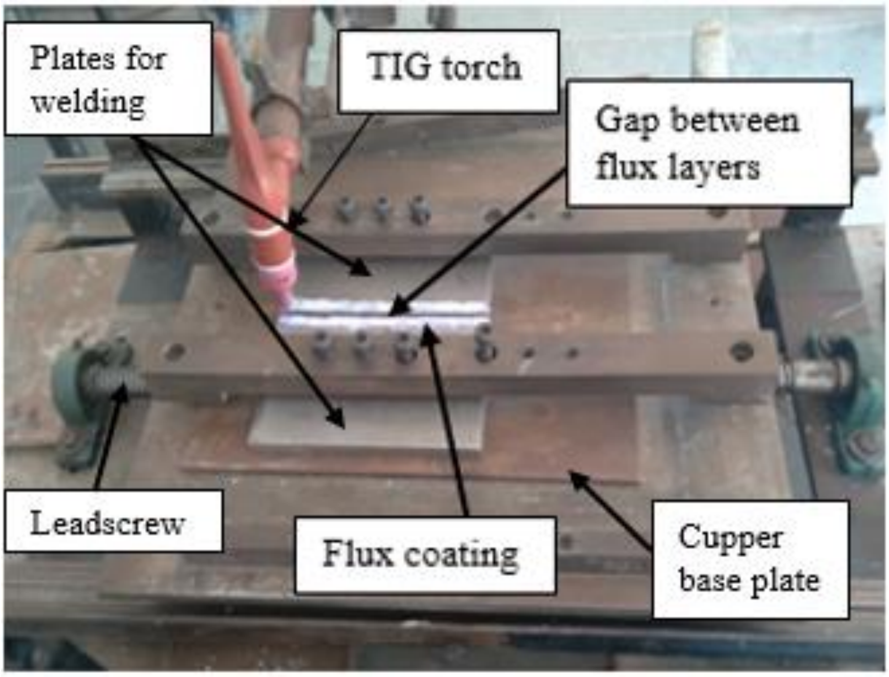

Figure 5.2 Flux applied in Flux Bounded TIG welding

Microstructure, microstructure and mechanical properties such as tensile strength, the microhardness of FB-TIG welded joint are studied as per standard procedure explained in chapter 3.

5.4 Influence of flux gap and flux on weld bead geometry

Flux gap has a substantial impact on weld depth and bead width (Jayakrishnan & Chakravarthy, 2017), (Neethu, Togita, Neelima, & Nair, 2019). The flux gap plays a very crucial role in increasing the penetration (Rückert, Perry, Sire, & Marya, 2014). At the lesser flux gap, a larger amount of flux will experience thermal desolation. Consequently, the concentration of surface-active elements (oxygen and sulfur) increases which leads to extensive reversal Marangoni convection. This phenomenon makes the arc column more constrict and thereby increases the energy density, this results in a higher D/W ratio in the weld metal.

In the present study, as discussed in chapter 4, SiO_2 flux gave the optimum results in A-TIG welding process. Thus to analyze the effect of flux gap, SiO_2 flux is adopted in FB-TIG welding process. Figure 5.3 shows that as the flux gap increases the penetration depth reduces. However, the effect on penetration depth doesn't follow a particular pattern. The penetration depth decreases when the flux gap rises from 2 mm to 3 mm and again increases at a 4 mm gap. However, beyond the flux gap of 5 mm, a reduction in penetration depth has been noticed in 2205 DSS weld. This is due to the absence of reversal Marangoni effect and poor arc constrictions. At 4 mm gap effect of constriction of the arc due to the insulating effect of flux dominates the effect of arc constriction due to negative ion and thereby increases the weld penetration. A similar observation is reported by Venkatesan et al. (2017) in 304L stainless steel FB-TIG weld. Moreover, TIG weld bead geometry is demonstrated in Figure 5.4 to compare the performance of FB-TIG weld metal.

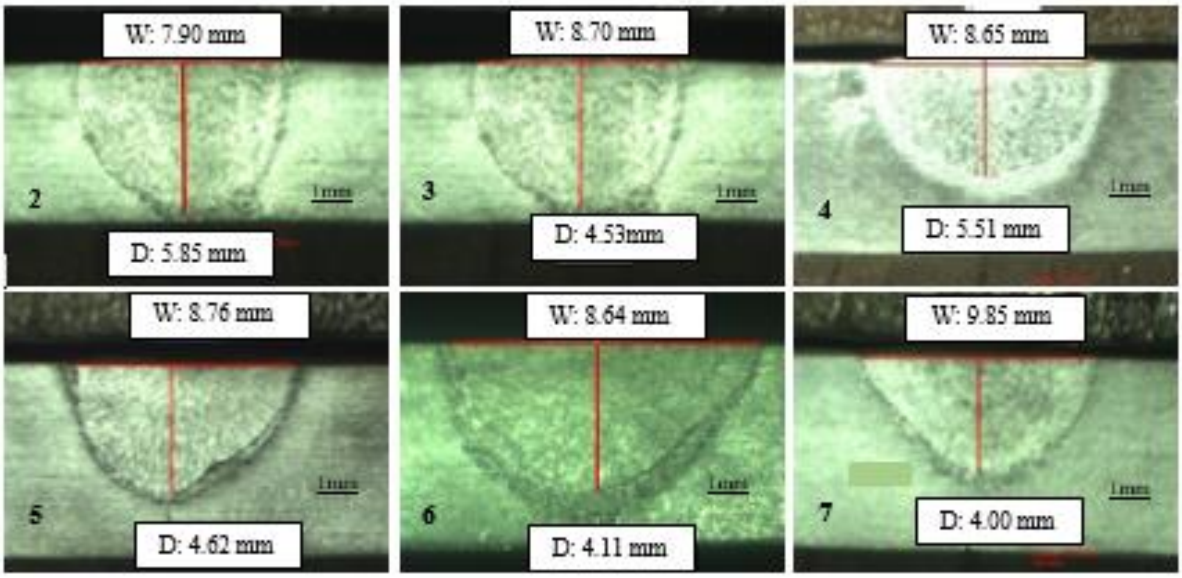

Figure 5.3 Flux bounded TIG weld bead geometry at varying the gap 2 to 7 mm with SiO_2 flux

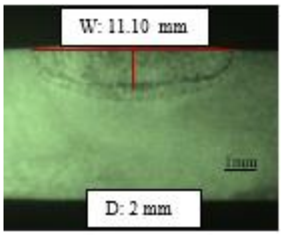

Figure 5.4 TIG weld bead geometry (D/W ratio: 0.18)

Figure 5.5 depicts that with a given set of weld parameters at a 2 mm flux gap, the highest D/W ratio (0.74) is achieved. This attributes to a high concentration of oxygen level in the weld pool due to the more amount of flux melted. Thereby, changing the temperature coefficient of surface tension from negative to a positive value which makes the Marangoni convection reverse. Moreover, constriction of the arc due to negative ions and the insulation effect of activated flux mutually decide the D/W ratio.

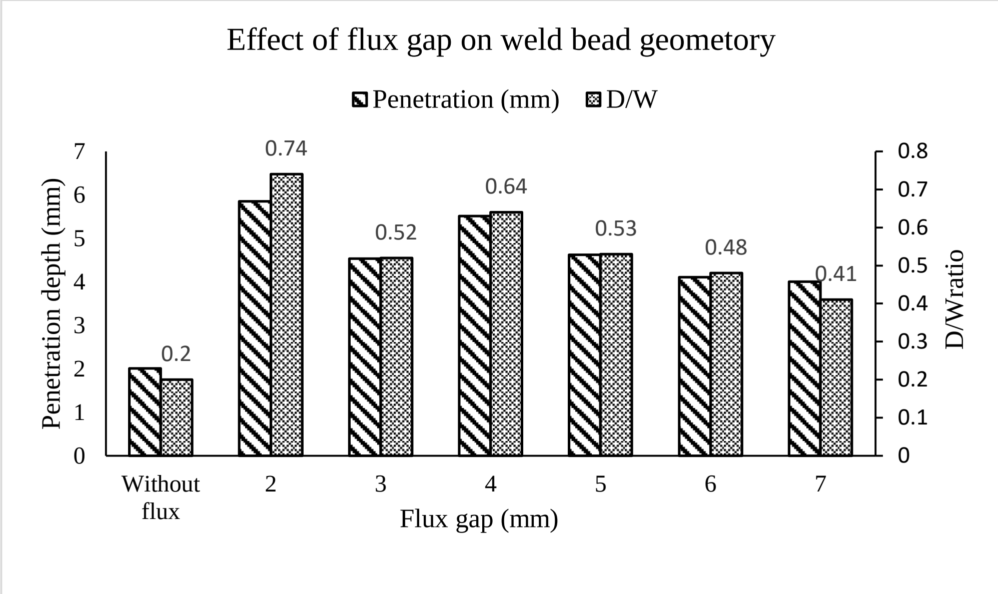

Figure 5.5 Influence of flux gap (with SiO_2 flux) on weld bead geometry of FB-TIG 2205 DSS weld

DOP also depends on the physical properties of flux i.e. melting and boiling point, change in free energy, composition and grain size. It is preferable to select the flux having a lower melting point and smaller grain size thereby lesser dissociation temperature. Which decides the oxygen level in the weld pool subsequently alters the weld bead geometry (Snow, 2002). In the present study, after finding the optimal flux gap (2mm) with SiO_2 flux, effect of TiO_2 and Cr_2O_3 flux on weld bead geometry is carried out. The maximum penetration achieved with SiO_2, TiO_2 and Cr_2O_3 is 5.9 mm, 4.97 mm and 5.19 mm respectively at 2 mm flux gap only as demonstrated in Figure 5.6.

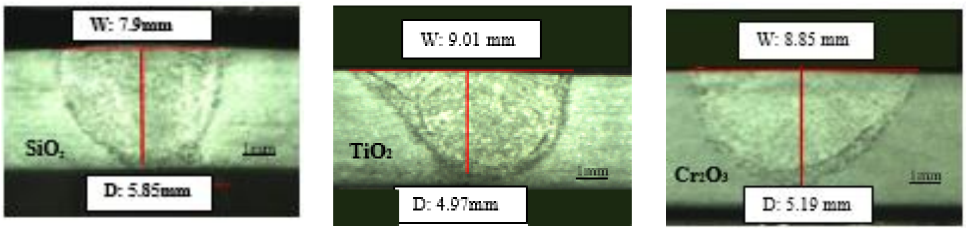

D/W: 0.74 D/W: 0.55 D/W: 0.58

Figure 5.6 Influence of different fluxes at 2 mm flux gap on weld bead geometry in FB-TIG 2205 DSS welds

The SiO_2 flux has a low melting point as well capability to release the highest amount of oxygen in the weld pool compared to the other two selected fluxes. Therefore, the highest penetration (5.85 mm) is achieved with SiO_2 flux. This is 193% higher than TIG weld penetration (2 mm). Similar, results were reported by Venkatesan et al. (2017) in FB-TIG weld and Shyu and Huang (2008) in A-TIG weld of 304 stainless steel. Hence, to measure the variation of weld heat input (current of weld) on microstructure and mechanical properties, SiO_2 flux with a 2 mm flux gap is selected.

5.5 Influence of heat input (welding current) on weld bead geometry and microstructure

Welding current plays a vital role to identify the quantity of heat input in weld pool which decides the welds pool shape and size (Wu & Gao, 2002). The amount of heat flux density at weld joint depicted the weld D/W ratio, cross-section area of weld joint which governs the quality of the weld.

In this study to analyze the effect of heat input on FB-TIG weld, the current is varied from 160 amps to 235 amps at the interval of 25 amps with 2 mm flux gap at the aforementioned weld parameters. The variation of ferrite content and change in macrostructure at different heat inputs are shown in Table 5.1. Figure 5.7 demonstrates the effect of welding current (heat input) on weld bead geometry. An increase in current, increase the heat input and temperature gradient which enhance the reversal of Marangoni convection. Subsequently, higher penetration depth with fewer variations in bead width has been observed. Increase in heat input leads to full penetration. However, it makes the weld pool wider and at 235amps current, extra metal deposition is observed at weld bead. The highest D/W ratio is reported with 210 amps current further increase in current leads to higher bead width and thereby reducing the D/W ratio.

Table 5.1 Consequence of heat input on macrostructure on FB-TIG 2205 DSS weld joint

Sr. No.	**Current (Amps)**	**Heat input (KJ/mm)**	**Ferrite Number (FN)**	**Macrostructure of weldments**
1.	160	1.14	75	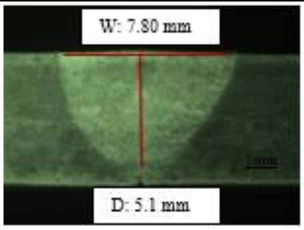
2.	185	1.34	73	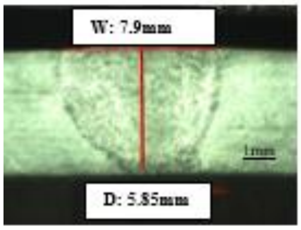
3.	210	1.53	71.5	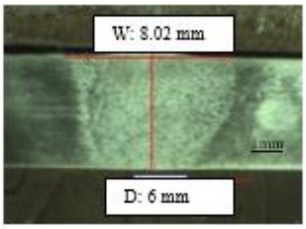
4.	235	1.73	69	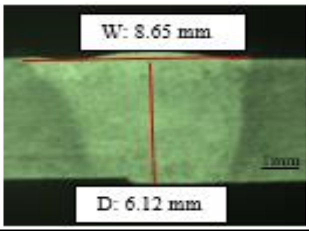

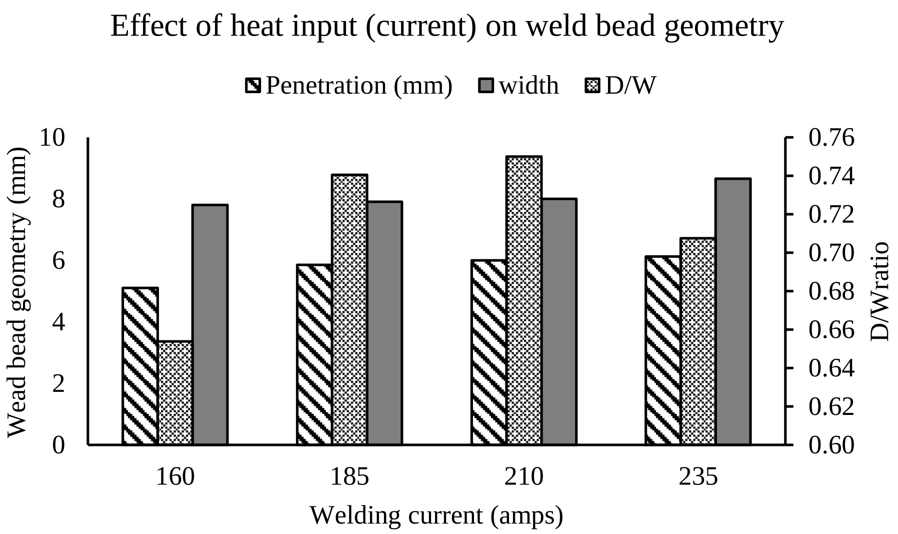

Figure 5.7 Influence of heat input (welding current) on FB-TIG 2205DSS weld bead geometry

Figure 5.8 (a) shows 2205 DSS base material microstructure having islands of grey color austenite in a black color ferrite matrix. The DSS microstructure consists of an almost equal portion of austenite and ferrite phases (Mourad, Khourshid, & Sharef, 2012). DSS weld metal solidified as complete ferrite phase. Figure 5.8 (b) TIG weldment observed the epitaxial growth and both austenite and ferrite, are present at grain boundary with uniform distribution of the delta ferrite matrix. A similar observation is reported by Tathgir et al. (2019) in 2205 DSS TIG weld. The amount of ferrite form after the solidification of DSS weld can be controlled by cooling rate and heat input during welding (Garzón & Ramirez, 2006). Figure 5.8 (a), (b) demonstrates that the delta ferrite number increases from 62 FN to 82 FN after TIG weld. This is attributed to lower heat input, higher rate of cooling, the conversion of delta ferrite to austenite is incomplete, which results in a richer amount of ferrite in the weldment. A similar study was reported by Chern et al. (2011) in 2205 DSS TIG weldments. The allomorphs of austenite are Widmanstätten side-plates, grain boundary and intergranular precipitate formation depending upon the heat input and temperature cycles (Sathiya, Aravindan, Soundararajan, & A., 2009).

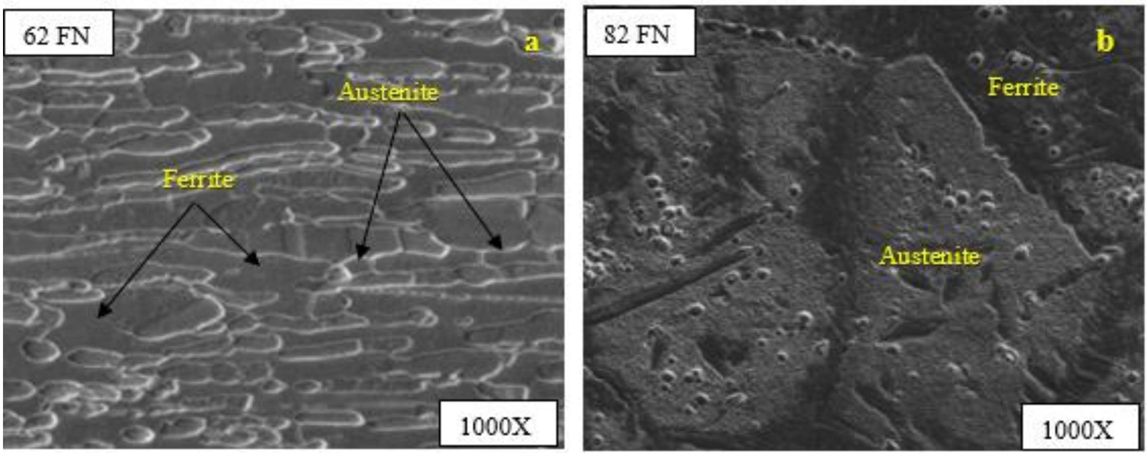

Figure 5.8 Microstructure of (a)2205 DSS base material (b) TIG weld metal

In this study, the effect of the maximum and minimum heat input on FB-TIG weldments microstructure has been reported. At these heat input conditions the grain boundary austenite, Widmanstätten austenite and the intergranular austenite in ferrite matrix are observed. However, the intergranular austenite may form during multipass welding as it required a higher driving force (high degree of undercooling) compare to Widmanstätten austenite and grain boundary austenite (Garzón & Ramirez, 2006). Therefore, less growth of intergranular austenite has been observed compared to the other two types of austenite as presented in Figure 5.9 (a),(b). At higher temperatures, the diffusion rate is faster, which results in higher amounts of Widmanstätten austenite.

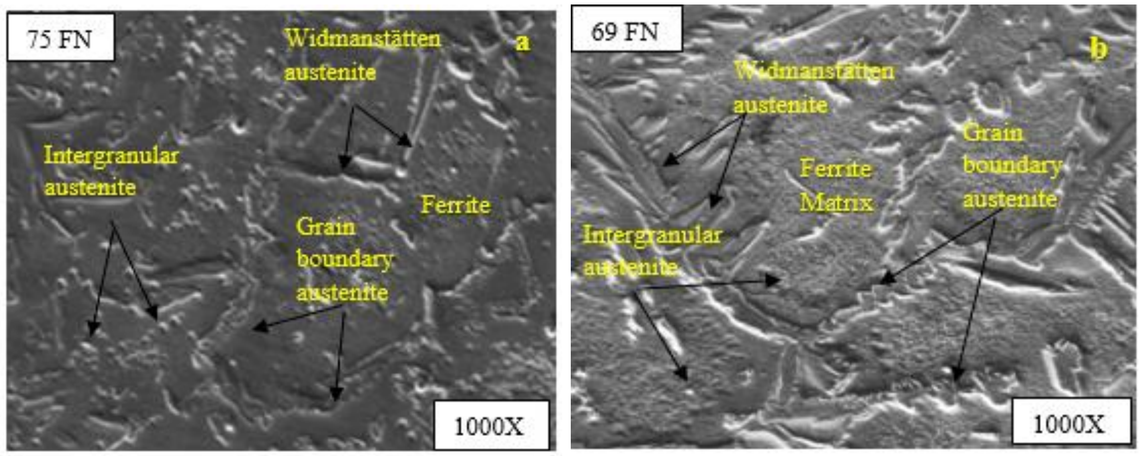

Figure 5.9 Microstructure at (a) minimum heat input 160 A current (1.14 KJ/mm) (b) maximum heat input 235A current (1.73 KJ/mm) of FB-TIG 2205DSS weld metal

In FB-TIG weld, at low and high heat input weld conditions, delta ferrite number, 75 FN and 69 FN are observed respectively which is lesser compared to TIG weldments. This is because the increase in heat density (reduce the cooling rate) is due to activated flux. To achieve the equilibrium phase conversion of delta ferrite to austenite phase is almost complete, thus the reduction in the ferrite content is observed than TIG weld. The richer amount of Widmanstätten austenite formation is reported at high heat input due to the energy-rich arc welding in 2205 DSS as shown in Figure 5.9(b).

5.6 Effect of heat input on mechanical properties

5.6.1 Tensile strength

To understand the influence of heat input on mechanical properties, the tensile study is performed on FB-TIG 2205 DSS welds. All tensile test specimens failed from the fusion zone and measured tensile properties are shown in Figure 5.10. TIG welded specimen showed tensile strength of 700 MPa which is less than base metal (720MPa). This reduction in tensile strength is owing to less heat input, (higher the cooling rate) consequently higher the amount of delta ferrite (82 FN). In FB-TIG weld joint, at low heat input (1.14 KJ/mm) insufficient penetration is reported consequently, an unacceptable weld profile, results in less tensile strength. By increasing the heat input, improvement in tensile strength has been reported as demonstrated in Figure 5.10. The maximum tensile strength (772 MPa) is observed at 210 A welding current (heat input 1.53 KJ/mm) which is 10% higher than TIG weld. This is attributed to complete and secure penetration with a maximum depth to width ratio (0.75). Moreover, at the higher energy input Widmanstätten austenite is more abundant in composition with lesser delta ferrite than TIG weld as depicted in Figure 5.9 (b) which is responsible for higher tensile strength in FB-TIG 2205 DSS weld. This shows the good correlation between the tensile properties and microstructure.

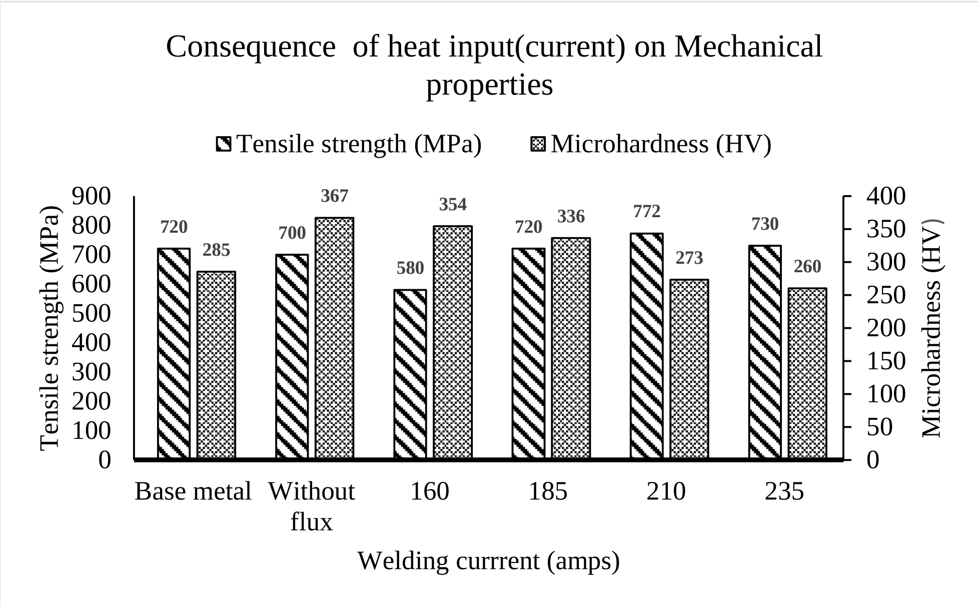

Figure 5.10 Influence of heat input on mechanical properties of FB-TIG DSS weldments

5.6.2 Microhardness

Variation of heat input affects the cooling rate and austenite: ferrite ratio and thereby affects the microhardness (Khoshnaw, 2021). TIG and FB-TIG 2205 DSS all weldments under different heat input, Vickers microhardness is measured (100 gf load) as demonstrated in Figure 5.10. The TIG welding microhardness is comparatively higher than FB-TIG weldments due to higher cooling rate smaller the grain size and higher delta ferrite (82 FN) formation. The average grain size of base metal is noticed 16 microns (ASTM E112/E 1382-91) whereas, TIG weld heat-affected zone is observed as ̃7.75 microns. Reduction in grain size and higher ferrite number confirmed the higher hardness (367HV) in TIG weld metal. In FB-TIG weld, higher heat input tends to adverse effect on the weld strength. As the current increases heat input increases, thereby lowering the cooling rate consequently higher the grain size. Figure 5.11 shows the microhardness profile across the entire width of the weld cross-section of FB-TIG weld at different heat inputs.

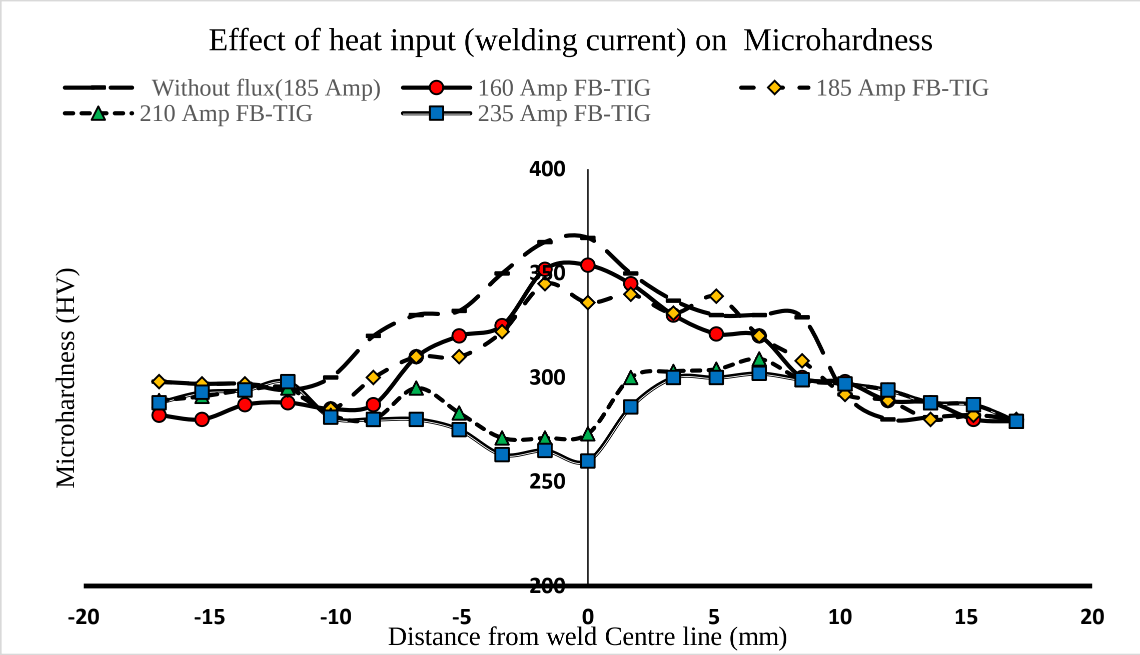

Figure 5.11 Microhardness of TIG (at 185 A current) and FB-TIG weld joint at different heat input

At maximum heat input, 235A welding current (1.73 KJ/mm) measured ferrite number is 69 FN and average grain size is 87 microns which is responsible for less microhardness 260 HV. Moreover, at this condition, microhardness is less than the base metal, this attributes to increase in grain size. Similarly, at minimum heat input, 160A welding current (1.14 KJ/mm) measured ferrite number is 75 FN and average grain size is 20 microns which leads to maximum hardness 354 HV. However, microhardness of all FB-TIG weld metals is less compared to TIG weld metal.

5.7 Summary

The observation made during experimental investigation on 2205 DSS TIG and FB-TIG weld joint are summarized below.

The flux gap plays a key role in weld penetration, at 2 mm flux gap the highest penetration depth 5.85 mm is obtained, which is 193% more than TIG weld under the same welding conditions. The SiO_2 flux reveals the more desirable weld penetration with a higher D/W ratio than other single component activated fluxes (TiO_2 and Cr_2O_3). With increase in heat input, penetration depth and D/W ratio increase. However, after the 210 A current further increases the current the D/W ratio decreases.

At minimum and maximum heat input conditions (FB-TIG weldments) reductions in delta ferrite, are reported as compared to TIG weld. This is attributed to increase in heat density due to activated flux. However, at high heat input, reduction in delta ferrite has been observed than minimum heat input along with significant growth of Widmanstätten austenite. In FB -TIG weld metal highest tensile strength 772 MPa is reported at 210 amps current. However, maximum microhardness 367 HV is observed in TIG weld at 185 amps current which is higher compared to all FB-TIG weldments due to reduction in grain size and excessive ferrite content in the weld metal. Though, with minimum heat input in FB-TIG weld, maximum microhardness 354 HV is obtained. From this study, it is concluded that during the welding low heat input condition should be avoided, because it would not have an adequate proportion of austenite in the weldments due to the rapid cooling rate. Therefore, weld metal would lose the stability between the austenite and ferrite phase, which is the characteristic of DSS.